

HYDROPHOBICALLY MODIFIED DEXTRAN ESTERS AS POTENTIAL EXTERNAL BIOCIDES

CRISTINA G. TUCHILUS¹, DALILA BELEI², ADINA COROABA³, MARIETA NICHIFOR⁴,
MAGDALENA CRISTINA STANCIU^{4*}

¹“Grigore T. Popa” University of Medicine and Pharmacy, Department of Microbiology, Faculty of Medicine, 16 University Street, 700115, Iași, Romania

²“Al. I. Cuza” University of Iași, Faculty of Chemistry, Department of Organic Chemistry, 11 Carol I Avenue, 700506, Iași, Romania

³“Petru Poni” Institute of Macromolecular Chemistry, Centre of Advanced Research in Bionanoconjugates and Biopolymers, 41A Grigore Ghica Voda Alley, Iași, 700487, Romania

⁴“Petru Poni” Institute of Macromolecular Chemistry, Department of Natural Polymers, Bioactive and Biocompatible Materials, 41 A Grigore Ghica Voda Alley, 700487, Iași, Romania

*corresponding author: cstanciu@icmpp.ro

Manuscript received: February 2022

Abstract

Amphiphilic dextran-based esters were synthesized by coupling several disubstituted 1,2,3-triazole derivatives on the polysaccharide. The polymers were characterized by elemental analysis and spectroscopy measurements: X-ray photoelectron (XPS), Fourier transform infrared (FTIR), carbon-13 nuclear magnetic resonance (¹³C NMR). Triazole derivatives and their corresponding dextran esters showed a moderate to good antimicrobial activity, the antifungal activity being stronger than the antibacterial one. Halogenated polymers proved to be potential external biocides due to their both bactericidal and fungicidal activity.

Rezumat

Esterii amfifili bazați pe dextransi au fost sintetizați prin cuplarea pe polizaharida a mai multor derivați disubstituiți ai 1,2,3-triazolului. Polimerii au fost caracterizați prin analiza elementală și măsurători spectroscopice (de fotoelectroni cu raze X - XPS, în infraroșu cu transformată Fourier - FTIR, rezonanță magnetică nucleară carbon-13 - ¹³C RMN). Derivații de triazol și esterii dextransului corespunzători au prezentat o activitate antimicrobiană moderată spre bună, activitatea antifungică fiind mai puternică decât cea antibacteriană. Polimerii halogenați s-au dovedit a fi produse potențiale biocide externe datorită activității lor bactericide și fungicide.

Keywords: dextran esters, 1,2,3-triazole derivatives, antimicrobial activity

Introduction

The number of deaths, caused by infections due to bacteria, viruses and fungi, is continuously growing. The elimination of microorganisms is difficult due to their fast and facile mutation [34, 39, 53, 57]. Therefore, it is essential to create new antimicrobial agents for treating the increasing resistance of microorganisms. Antimicrobial polymers represent a class of therapeutics which combated the microbial infections. In contrast with low-molecular-weight antimicrobial agents, the polymeric ones have the benefit that they are non-volatile and chemically stable, do not penetrate by skin, have lower toxicity and long-term activity [30, 59]. Based on the type of polymeric system, antimicrobial polymers can be classified [7]: (1) biocidal polymers, with intrinsic antimicrobial activity; (2) polymeric biocides, which have biocide molecules attached on the polymer backbone; and (3) biocide-releasing polymers, having biocide molecules included in a polymeric matrix.

1,2,3-triazoles and their derivatives, synthesized in the last decades by “click chemistry” [1, 48, 55], have various pharmacological activities, such as: anticancer [14, 15, 24], anti-HIV [25, 37, 64], antiviral [9, 19, 32], antimycobacterial [3, 4, 20, 42], antifungal [2, 13, 29], antidiabetic [5, 18, 49], antitubercular [41, 46, 50], anti-malarial [8, 10, 43], anti-inflammatory [38, 45]. These N-heterocyclic derivatives linked to carbohydrates have captured broad attention, due to their increased solubility and biological activity [17, 28, 54]. Thus, new antimicrobial products based on 1,2,3-triazole derivatives conjugated with monosaccharides (D-glucose, D-galactose, D-mannose, D-fructose [6] or D-galactose, D-glucose, D-xylose [16]) or polysaccharides (starch [52], lignocellulosic fibres [31]) were synthesised and evaluated concerning their antimicrobial activity. Recently, we synthesized new hydrophobically modified esters based on dextran, and we preliminary tested some of the obtained polymers against bacterial and yeast strains [51]. In the present work, a more in-depth study was made for establishing the correlation

between chemical structure and antimicrobial activity for a series of amphiphilic dextran esters. The polymers were synthesized by an one-pot procedure, consisting on the reaction between the polysaccharide and different 1,4-disubstituted-1,2,3-triazole-4-carboxylates *in situ* previously activated with N,N'-carbonyldiimidazole (CDI). The obtained polymers were characterized by elemental analysis, XPS, FTIR and NMR spectroscopy. Also, antibacterial and antifungal activity for 1,2,3-triazole-4-carboxylic acid derivatives and their corresponding polymers was tested against Gram-positive, Gram-negative bacteria and a pathogenic yeast by using disk diffusion method and broth microdilution method.

Materials and Methods

Materials

Dextran from *Leuconostoc* spp (Mr = 40,000 Da), N,N'-carbonyldiimidazole and pyrene were bought from Sigma-Aldrich and employed as received. Dimethylsulfoxide was dried on molecular sieves.

The microbial strains were achieved from the Culture Collection of the Department of Microbiology, Faculty of Pharmacy, "Gr. T. Popa" University of Medicine and Pharmacy, Iași, Romania.

Synthesis of dextran esters

Triazole carboxylates (**1a-f**) synthesis was previously described in detail [51] and implied two steps: "click" reaction between ethyl propiolate and organic azides in the presence of copper(II) sulphate pentahydrate and sodium L-ascorbate, followed by the alkaline hydrolysis (30% KOH aqueous solution) of obtained ethyl esters.

The synthesis of polysaccharide esters (**2a-f**) was carried out by esterification of dextran with derivatives (**1a-f**) activated *in situ* with CDI (Figure 1), using the procedure presented in our previous work [51], with some modifications.

Preparation of dextran ester **2a** is given as an example. 0.86 g (3.72 mmol) **1a**, solved in 8 mL of dry DMSO, reacted with 0.6 g (3.72 mmol) CDI under magnetic stirring, at r.t, for 8 h. Then, 0.15 g (0.93 mmol) dextran was added and the mixture was allowed to react under stirring, at 80°C, for 24 h. The product was separated by precipitation in 0.1 M aqueous solution of sodium bicarbonate for removing triazole derivative, and after it was filtered and washed several times with deionized water. Finally, dextran ester was dried at r.t. under vacuum. In the following, the atoms are numbered as shown in Figure 1. Dextran esters **2e** and **2f** contain a supplementary carbon atom, namely C¹³, attributed to methyl (product **2e**) or methoxy group (product **2f**) which are bound in para position of the benzene ring.

Methods

Preparation of polymeric self-aggregates

Polymeric self-associates were acquired by solving dextran ester in DMSO (0.1 g polymer/10 mL solvent)

followed by the drop-wise addition of DMSO polymeric solution to the twice its volume of Millipore water under magnetic stirring. The mixture was introduced into a dialysis bag (12 kDa cut-off) and dialyzed against Millipore water. The obtained colloidal solution was used by itself or after dilution for fluorometric analysis.

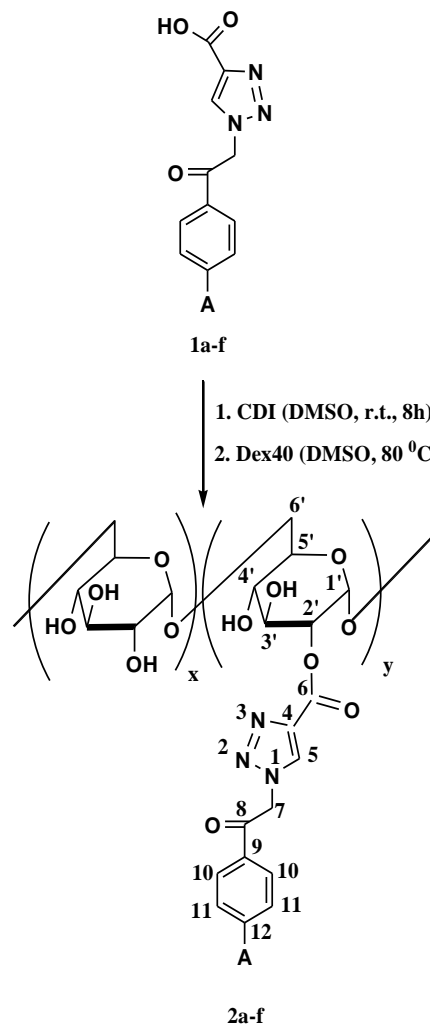


Figure 1.

Synthetic route for polymers **2a-f**
(A = H(**a**), F(**b**), Cl(**c**), Br(**d**), CH₃(**e**), OCH₃(**f**))

Chemical structure characterization

Elemental analysis (N%) was realized by using CHNS 2400 II Perkin Elmer analyser. XPS measurements were accomplished on a KRATOS Axis Nova (Kratos Analytical, Manchester, UK) which employed a monochromated Al K α source with 20 mA current and 15 kV voltage (300 W) and base pressure of 10⁻⁹ to 10⁻⁸ Torr in the sample chamber. The XPS survey spectra for the polymers were obtained with a resolution of 1 eV and a pass energy of 160 eV. The high resolution spectra for all the elements found from the survey spectra were achieved using a pass energy of 20 eV and a step size of 0.1 eV. Vision Processing (Version 2.2.10) software was employed for background subtraction (Linear-type), peak integration, fitting and

quantitative chemical analysis. All binding energies were referenced to the C1s peak at 285 eV. For XPS analysis, the powder polymers were put in a stream of nitrogen to eliminate non-adhered materials, and degassed for two hours. After, the samples were placed onto the sample stage by an aluminium powder support. FTIR spectra were registered with a Bruker Vertex 70 spectrophotometer on KBr pellets. ^{13}C NMR spectra were achieved in DMSO- d_6 with a Bruker Advance DRX 400C spectrometer (100 MHz), using tetramethyl silane (TMS) as internal reference compound.

Fluorescence experiments

The critical aggregation concentrations, CAC, of polymeric self-aggregates were obtained using pyrene as fluorescence probe. Polymeric concentrations, ranging from 1.3 mg/mL to 0.0007 mg/mL, were achieved by successive dilution of acquired self-associates in aqueous solution as explained in *Preparation of polymeric self-aggregates*. A known aliquot of pyrene solution in methanol ($7.0 \cdot 10^{-4}$ M) was put into a set of vials, succeeded by solvent vaporization. Thereafter, aqueous polymeric solutions of known concentration were inserted into the vials and the mixtures were preserved at r.t. for 24 h for system equilibration. The final concentration of the chromophore in vials was $7.0 \cdot 10^{-7}$ M. Steady-state fluorescence emission spectra were achieved with a LS 55 PerkinElmer fluorescence spectrometer, using an excitation wavelength of 337 nm, the excitation and emission slits widths being set at 5 and 2 nm, respectively. The emission spectra of the fluorophore, recorded between 350 and 550 nm, allowed the calculation of the polarity parameter (I_3/I_1) by knowing pyrene fluorescence intensities at 372 nm (I_1) and 383 nm (I_3).

Antimicrobial activity

Disc-diffusion method

Polymeric antimicrobial activity was examined using Gram positive bacterium (*Staphylococcus aureus* ATCC 25923), Gram negative bacteria (*Escherichia coli* ATCC 25922, *Pseudomonas aeruginosa* ATCC 27853) and a pathogenic yeast (*Candida albicans* ATCC 90028). The antimicrobial susceptibility tests were assessed using disk diffusion methods [11, 12]. Mueller Hinton agar (Oxoid) and Mueller-Hinton agar Fungi (Biolab) were inoculated with the suspensions of the tested microorganisms. Sterile stainless-steel cylinders (5 mm internal diameter; 10 mm height) were placed on the agar surface in Petri plates. Then, 100 μL of the evaluated products (**1a-f** and **2a-f**, as 1 wt% DMSO solutions) were adjoined into cylinders. The plates were kept 10 minutes at r.t. to obtain a homogeneous distribution of the compound in the medium and after, incubated at 35°C for 24 hrs. As reference antimicrobial drugs were used commercial available discs containing Ciprofloxacin (5 μg /disk), Fluconazole (25 μg /disk) and Voriconazole (1 μg /disc). After incubation, the diameters of inhibition zones were measured in mm, including disc size.

Broth microdilution method

Some polymers were evaluated for the minimal inhibitory concentration (MIC) and minimal bactericidal concentration (MBC) or minimal fungicidal concentration (MFC). Serial double dilutions of each extract were inoculated in cation-adjusted Mueller-Hinton broth (Oxoid) (CAMHB), with equal volumes of bacterial/yeast suspension (106 CFU/mL). MIC was the lowest concentration of extract where complete inhibition of visible growth was observed after 24 h of incubation at 37°C (for antibacterial test) and 24°C (for antifungal test). All the wells, showing complete inhibition of microorganisms' growth, were subcultured and incubated overnight at 37°C (for antibacterial test) and 24°C (for antifungal test). The highest dilution of extracts, which afforded the killing of 99.9% of tested microorganisms, was recorded as MBC/MFC. MIC and MBC/MFC of ciprofloxacin/fluconazole towards bacterial/yeast strains were also assessed.

Results and Discussion

Synthesis and chemical structure characterization

The polysaccharide esters, **2a-f**, were synthesized using a one-pot procedure (Figure 1). Triazole carboxylates, **1a-f**, reacted with the coupling agent (CDI) to provide the activated compounds (acylimidazoles) and two by-products: CO_2 and imidazole (Im). Further, the acylimidazolidine reacted *in situ* with dextran to obtain dextran ester.

The structural characterization of the polymers was performed by elemental analysis, XPS, FTIR and ^{13}C NMR spectroscopy. Elemental analysis and X-ray photoelectron spectroscopy proved the effective binding of triazole derivatives on dextran skeleton and enabled to obtain polymeric degree of substitution which values were higher than those previously reported [51] due to the higher molar ratio between the polysaccharide and 1,2,3-triazole derivative. DS were calculated by taking into account the nitrogen percent determined by elemental analysis. X-ray photoelectron spectroscopy was used only to prove esters formation and not for the evaluation of DS values because it is a surface analysis technique. XPS afforded the determination of the binding energies of all polymeric bonds and their relative intensity (%) (Table I).

The survey spectra and deconvoluted C1s, O1s and N1s spectra for both native dextran and one of the polymers, **2a**, used as an example, were showed in Figure 2. Thus, a distinct peak corresponding to the orbital of N (1s, 397 eV) (Figure 2a) was present in the wide spectrum of compound **2a**, due to the occurrence of 1,2,3-triazole derivative moiety in polymeric chemical structure, while no peak from N1s could be seen for pure dextran. Peaks from C (1s, 284.44 eV) and O (1s, 528.75 eV), O (2s, 23.31 eV), O (KLL, 974.76 eV) were found in both survey spectra of neat polysaccharide and dextran ester. The C1s spectrum of

pristine dextran (Figure 2b) revealed a main peak at 286.5 eV which could be assigned to C–O bond. Two small peaks at 285 eV and 287.8 eV could also be observed and were attributed to the C-C/C-H and C-O-C bonds which occurred in neat polysaccharide structure. The O1s spectrum of pure polysaccharide (Figure 2c) showed two peaks. The main one, at 532.7 eV, could be ascribed to the O–C bond. The

second one, at 533.1 eV, was smaller and it confirmed the existence of C-O-C bond in native dextran. In contrast to dextran XPS spectrum, two new and small peaks for the C 1s signal appeared in the spectrum of ester **2a** at binding energies (BEs) of 285.9 and 289.2 eV indicating C-N and O-C=O bonds formation (Figure 2d).

Table I

Binding energies (eV), relative intensity (%) and their assignment for dextran esters

Polymer code	C 1s		O 1s		N 1s	
	BE (eV)	Assignment	BE (eV)	Assignment	BE (eV)	Assignment
2a	285 (32.47%)	C-C/C-H	532.4 (42.96%)	O-C	400.3 (36.07%)	N-N
	285.9 (7.09%)	C-N				
	286.5 (43.63%)	C-O				
	287.8 (12.95%)	C=O/ C-O-C				
	289.2 (3.86%)	O-C=O				
2b	285 (20.33%)	C-C/C-H	532.3 (40.54%)	O-C	400 (42.49%)	N-N
	285.7 (6.45%)	C-N				
	286.3 (36.68%)	C-O				
	287.5 (23.20%)	C=O/ C-O-C				
	288.5 (9.19%)	C-F				
	289.5 (4.15%)	O-C=O				
2c	285 (34.64%)	C-C/C-H	531.7 (19.69%)	O-C	399.8 (32.43%)	N-N
	285.6 (6.18%)	C-N				
	286.3 (42.42%)	C-O/C-Cl				
	287.7 (12.76%)	C=O/ C-O-C				
	289.1 (4%)	O-C=O				
2d	285 (23.27%)	C-C/C-H	532.2 (40.5%)	O-C	400.2 (43.53%)	N-N
	285.8 (5%)	C-N				
	286.5 (35.73%)	C-O/C-Br				
	287.9 (27.23%)	C=O/ C-O-C				
	289.4 (8.77%)	O-C=O				
2e	285 (33.68%)	C-C/C-H	531.5 (12.2%)	O-C	400.1 (49.87%)	N-N
	285.7 (6.08%)	C-N				
	286.5 (44.63%)	C-O				
	287.8 (12.52%)	C=O/ C-O-C				
	289.2 (3.09%)	O-C=O				
2f	285 (23.26%)	C-C/C-H	531.9 (19.36%)	O-C	399.9 (38.16%)	N-N
	285.7 (6.3%)	C-N				
	286.5 (52.69%)	C-O				
	287.7 (13.67%)	C=O/ C-O-C				
	289.2 (4.08%)	O-C=O				

The O 1s spectrum of polysaccharide-based polymer showed a new broad peak at 533.8 eV pointing out the formation of C=O bond (Figure 2e). The N 1s spectrum of product **2a** revealed three intensive peaks at BEs of 400.3, 401 and 402 eV relative to N-N, N-C and N=N bonds formation, respectively (Figure 2f). DS values, expressed in moles of 1,2,3-triazolic group *per* 100 glucopyranosidic units (U_{GI}) were determined with equation (1) by considering the nitrogen content provided by elemental analysis (Table II).

$$DS = \frac{162 \times \%N}{(100 \times 3 \times 14) - [\%N \times (M_S - 1)]} \times 100, \text{ mol}/100 U_{GI} \quad (1),$$

where, %N is the nitrogen percent determined by elemental analysis; 14 is elemental mass for N and 162 is molar mass of glucopyranoside unit of dextran; M_S is the molecular weight of N-heterocyclic pendant

group (-CO-Tr-CH₂-CO-C₆H₄-A) (Tr =1,2,3-triazole) (A=H, F, Cl, Br, CH₃, OCH₃).

Polymers were achieved by nucleophilic acyl substitution between dextran and acyl compound obtained by the reaction between N-heterocycle derivatives and the coupling agent. Moderate DS values of the polymers could be explained by steric hindrance exerted between two bulky groups (-Tr-CH₂-CO-C₆H₄-A and -Im) bound to the carbonyl group of acylimidazolidine in the first step of nucleophilic substitution followed in the second stage by elimination of imidazole with the formation of dextran esters. Degree of substitution values increased with the augmentation of triazole derivatives solubility in the reaction medium [47], as follows: $DS_{Dex-T-CH_3} < DS_{Dex-T-H} < DS_{Dex-T-Br} < DS_{Dex-T-Cl} < DS_{Dex-T-F} < DS_{Dex-T-OCH_3}$.

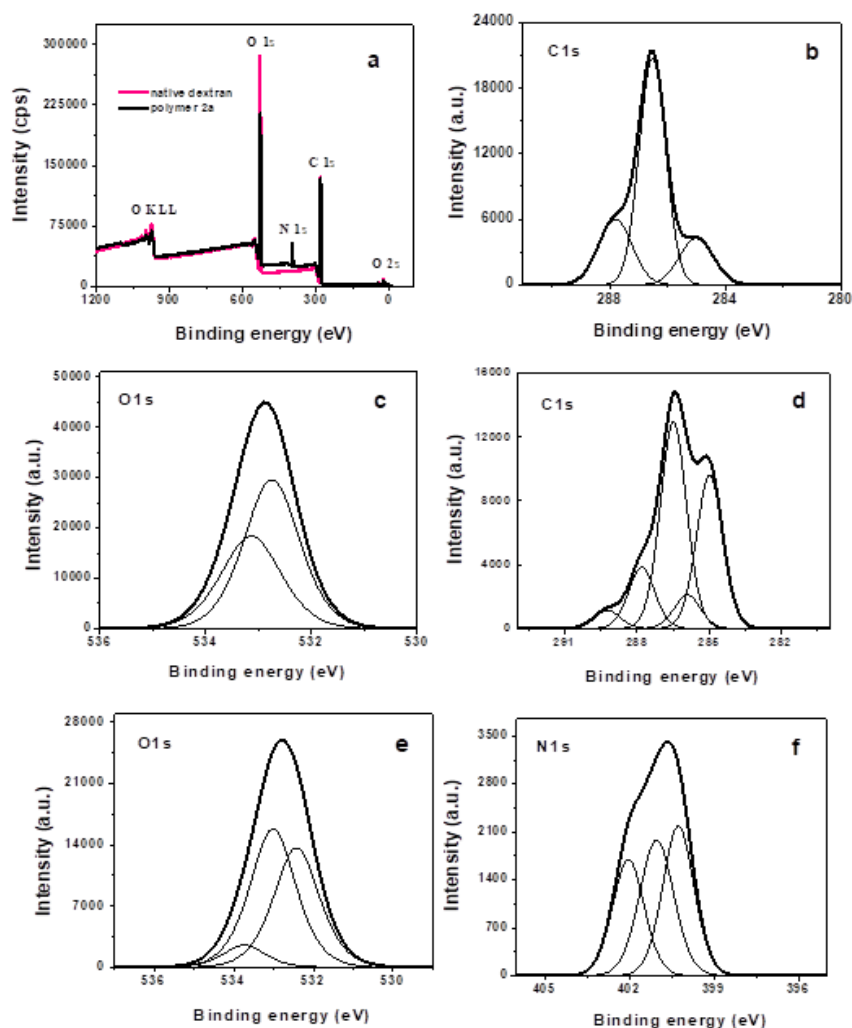


Figure 2.

The survey spectra for pristine dextran and polymer **2a** and deconvoluted profiles for pure dextran: (b) C 1s, (c) O 1s and polymer **2a**: (d) C 1s, (e) O 1s, (f) N 1s

Table II
Characteristics of polymers **2a-f**

Polymer code	Substitution degree (mol/100 U _{GI}) [a]	Weight content of hydrophobic groups (wt %)	CAC (mg/mL)
2f	87	58.4	0.020
2b	82	54.1	0.038
2c	77	55.4	0.027
2d	71	60.3	0.016
2a	67	47.0	0.058
2e	65	49.3	0.046

FTIR and NMR were also used for the characterization of dextran-based polymers, the spectral data of the polymers **2a-f** being collected in Table III.

FTIR spectroscopy proved the successful attachment of 1,2,3-triazolic moieties on polysaccharide skeleton by the comparison of FTIR spectrum (Figure 3c) of one of the polymers, **2a**, with those of its corresponding disubstituted triazole, **1a** (Figure 3b) and native dextran (Figure 3a).

So, a new signal in the range 1732 - 1735 cm⁻¹, attributed to the C=O_{ester}, appeared in FTIR spectrum of dextran

ester while the signal for C=O_{acid} (1682 - 1698 cm⁻¹ [51]) disappeared. Also, in FTIR spectrum of the polymer **2a** could be seen mutual stretching adsorption bands with those that occurred in FTIR spectra of pure dextran and triazole derivative **1a**. Thus, common signals with neat dextran were those for O-H_{alcohol} (3415 - 3428 cm⁻¹) and C-H (2924 - 2935 cm⁻¹) while mutual adsorption bands with 1,2,3-triazole derivative were those for C=C_{triazole} (1574 - 1598 cm⁻¹) and C=O_{ketone} (1689 - 1705 cm⁻¹).

Table III

FTIR and ^{13}C NMR spectral data of dextran polymers

Spectral analysis	Bound/Carbon atom	Polymer code					
		2a	2b	2c	2d	2e	2f
FTIR ν (cm^{-1})	O-H	3415	3425	3415	3428	3424	3418
	C-H	2932	2924	2935	2933	2925	2929
	C=O _{ester}	1735	1734	1734	1732	1735	1735
	C=O _{ketone}	1702	1703	1705	1704	1697	1689
	C=C _{triazole}	1597	1598	1585	1587	1582	1574
	C-F	-	1161	-	-	-	-
	C-Cl	-	-	1095	-	-	-
	C-Br	-	-	-	1071	-	-
^{13}C NMR δ (ppm)	C _{arom} -O-C _{aliph}	-	-	-	-	-	1047
	C ⁷	56.3	56.3	56.2	56.2	56.3	56.2
	C ^{6'}	65.2	65.5	65.3	65.1	65.8	65.4
	C ^{2'} -C ^{5'}	67.1-76.6	67.2-76.6	67.1-76.4	66.2-76.6	67.1-76.6	67.2-73.5
	C ^{2''}	76.3	76.7	76.5	76.6	76.4	76.3
	C ^{1''}	95.6	95.5	95.2	95.3	95.6	95.6
	C ^{1'}	98.7	98.3	98.3	98.4	98.1	98.4
	C ¹¹	128.1	116.2	128.7	132.4	129.7	128.2
	C ¹⁰	129.6	131.6	129.8	130.2	128.4	130.3
	C ⁵	130.9	130.6	130.9	130.9	130.8	130.7
	C ¹²	134.8	164.8	133.5	128.7	131.5	159.3
	C ⁴	137.8	138.7	133.7	138.5	138.6	138.5
	C ⁹	141.3	144.6	140.5	140.8	144.8	140.7
	C ⁶	159.6	160.4	159.8	159.7	160.2	160.2
C ⁸	191.8	190.2	191.2	191.3	191.3	189.7	
C ¹³	-	-	-	-	21.3	58.7	

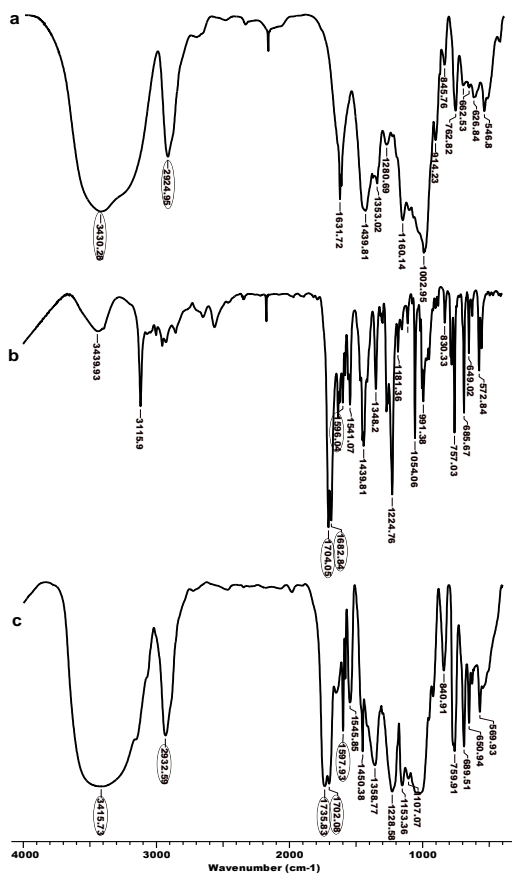


Figure 3.

FTIR spectra of native dextran (a), triazole derivative **1a** (b) and polymer **2a** (c)

^{13}C NMR spectroscopy was used for the characterization of dextran-based polymers because of a limited separation of polymeric peaks in ^1H NMR spectra. ^{13}C NMR spectrum of polymer **2a** (Figure 4c) was compared with those of its corresponding 1,2,3-triazole-4-carboxylic acid **1a** (Figure 4b) and pristine dextran (Figure 4a). ^{13}C NMR spectra revealed that the attachment of 1,2,3-triazole group on dextran backbone happened preferentially at the hydroxyl group bound to the second carbon of the polysaccharide ring by the presence of the signal corresponding to substituted second carbon of the polysaccharide ring (C^{2''}) at 76.6 ppm whilst the picks for substituted C^{3'} or C^{4'} could not be found. Additionally, the occurrence in ^{13}C NMR spectrum of dextran ester **2a** of the signals at 95.37 and 98.27 ppm showed that the substitution reaction at the hydroxyl group bound to C² was incomplete. The pick from 95.37 ppm corresponded to the first carbon of glucopyranosidic unit which was adjacent to substituted second carbon (C^{1''}) while the pick from 98.27 ppm belonging to the first carbon next to unsubstituted second carbon (C^{1'}). The signals, belonging to carbon atoms of 1,2,3-triazole moiety, could be located in ^{13}C NMR spectra of compounds **1a** and **2a** at: 56.3 (C⁷), 128.1 (C¹¹) 129.6 (C¹⁰), 130.9 (C⁵), 134.8 (C¹²), 137.8 (C⁴), 141.3 (C⁹), 159.6 (C⁶) and 191.8 ppm (C⁸). Also, the picks corresponding to carbon atoms of dextran unit could be seen in ^{13}C NMR spectra of native polysaccharide

(Figure 4a) and dextran ester (Figure 4c) at: 66 (C^{6'}), 70.0 (C^{4'}), 70.4 (C^{5'}), 71.8 (C^{2'}) and 73.3 ppm (C^{3'}).

Critical aggregation concentration of polymeric self-aggregates

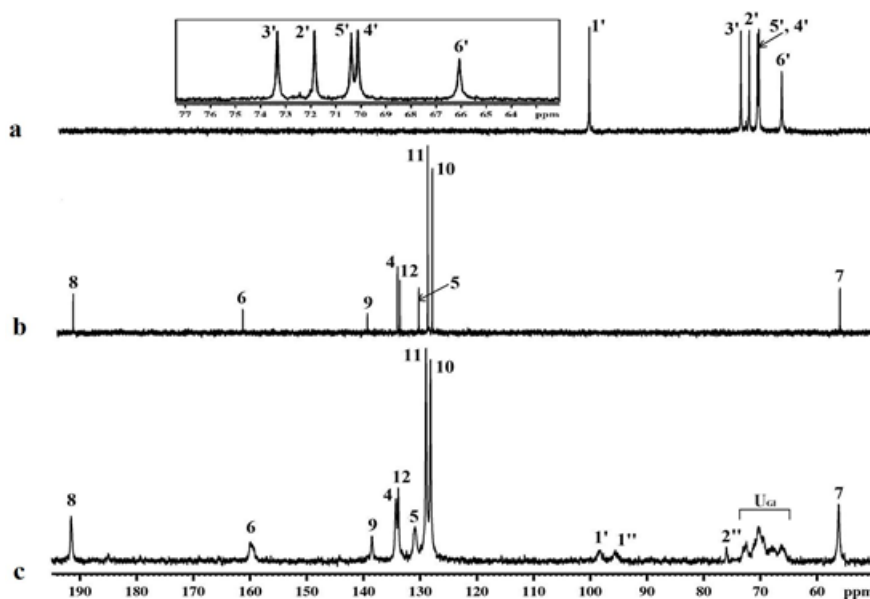


Figure 4.

¹³C-NMR spectra of pure dextran (a), triazole derivative **1a** (b) and polymer **2a** (c)

Hydrophobically-modified polymers **2a-f** could self-assemble in aqueous solution and their capacity to associate was studied by fluorometry using pyrene as fluorescence probe. It is known that pyrene polarity parameter (I_3/I_1), which is ratio of intensity of its third (382 nm) (I_3) to first (373 nm) (I_1) vibronic peaks, is a measure of the local polarity of the chromophore microenvironment. The interception of two straight lines afforded the determination of polymeric critical aggregation concentrations (Figure 5) and these values depended on the weight content of hydrophobic 1,2,3-triazole moieties (wt%).

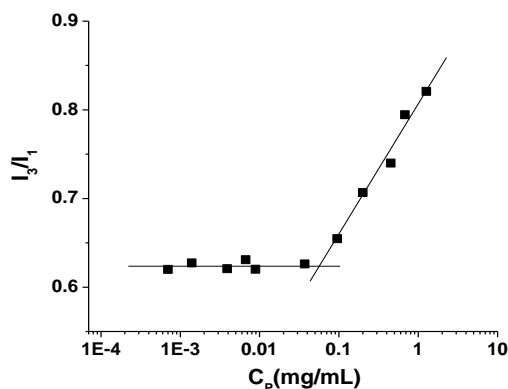


Figure 5.

Variation of pyrene polarity parameter with the polymer concentration for dextran ester **2a**

CAC values increased with the decrease of wt (%) (Table II). Critical aggregation concentrations of

compounds **2a-f** were in agreement to those related to other amphiphilic dextran-based polymers with the same molar mass of the polysaccharide and having as side chains different lipophilic moieties, such as: tocopherol succinate [26], stearic acid [62] or retinal [61].

Figure 5, representing the variation of polarity parameter *versus* the concentration of dextran ester **2a**, showed almost unchanged values of I_3/I_1 at low polymer concentrations while I_3/I_1 values increased with the augmentation of polysaccharide ester concentrations. This behaviour is due to the progressive embedding of pyrene molecules in polymeric hydrophobic microdomains which were obtained as a result of the self-organization of amphiphilic polymer in aqueous medium.

Antimicrobial activity

The antimicrobial activity of substituted 1,2,3-triazole-4-carboxylic acids, **1a-f**, and their corresponding dextran-based polymers, **2a-f**, were assessed against four different strains which are frequently connected with infections: a Gram-positive bacterium (*Staphylococcus aureus* ATCC 25923), two Gram-negative bacteria (*Escherichia coli* ATCC 25922, *Pseudomonas aeruginosa* ATCC 27853) and a pathogenic yeast (*Candida albicans* ATCC 90028). Antimicrobial activity was qualitatively estimated by using antimicrobial susceptibility test [27] which afforded the evaluation of the inhibition zone diameter, the results being collected in Table IV.

As positive control for antimicrobial activity was used ciprofloxacin and for antifungal activity, fluconazole and voriconazole. The examined compounds **1a-f** and

2a-f showed antimicrobial activity against both Gram-positive bacterium and pathogenic yeast. Conversely, all the products did not reveal any Gram-negative bacteria growth inhibition in the employed concentration range. That is in accordance with earlier studies which indicated that Gram-positive bacteria are more receptive to small or macromolecular products than Gram-negative bacteria due to their mesh-like peptidoglycan layer, located outside the plasma membrane, which can be easily traversed by different biocides [21, 22]. Instead, in the case of Gram-negative bacteria, the peptidoglycan layer is sandwiched between an inner cell membrane and an outer membrane which make extremely difficult the passive diffusion of the compounds [21, 22]. This behaviour is similar to other antimicrobial small molecules or polymers which contained 1,2,3-triazole moieties in their chemical structure [16, 63]. It is known that 1,2,3-triazoles are antimicrobial agents

per se, because they can inhibit synthesis of the cell membrane, cell wall, and nucleic acids of bacteria [35].

The antimicrobial action is generally caused by ionic and hydrophobic interactions between the biocide and the outer phospholipid membrane of the microorganism [40]. The ionic attractions were exerted between the partial positive charge of N-heterocycle-containing products, induced by electron-withdrawing effect of carboxylic group linked directly to C4 of 1,2,3-triazolic ring, and negatively charged outer cellular membrane of bacteria or fungi while the hydrophobic forces were established between their lipophilic segments. As a result of both ionic and hydrophobic forces, several defects in the membrane integrity with loss of cytoplasmic constituents were determined, causing the death of the microorganism [23, 36].

Table IV

Antibacterial and antifungal activities of the compounds **1a-f** and **2a-f**

Polymer sample	Diameter of inhibition zones (mm)			
	<i>S. aureus</i> ATCC 25923	<i>E. coli</i> ATCC 25922	<i>P. aeruginosa</i> ATCC 27853	<i>C. albicans</i> ATCC 90028
1a	11.0 ± 0.00	0	0	16.0 ± 0.00
1b	15.1 ± 0.05	0	0	17.1 ± 0.05
1c	14.0 ± 0.00	0	0	18.0 ± 0.00
1d	14.0 ± 0.00	0	0	16.0 ± 0.00
1e	12.1 ± 0.05	0	0	15.3 ± 0.57
1f	13.1 ± 0.05	0	0	15.0 ± 0.00
2a	14.0 ± 0.00	0	0	17.0 ± 0.00
2b	20.0 ± 0.00	0	0	20.1 ± 0.05
2c	18.0 ± 0.00	0	0	18.1 ± 0.05
2d	17.0 ± 0.00	0	0	17.8 ± 0.00
2e	13.7 ± 0.57	0	0	16.0 ± 0.05
2f	14.6 ± 0.05	0	0	15.0 ± 0.05
Ciprofloxacin (5 µg/disc)	32.7 ± 0.00	32.1 ± 0.05	32.0 ± 0.00	NT*
Fluconazole (25 µg/disc)	NT*	NT*	NT*	30.0 ± 0.00
Voriconazole (1 µg/disc)	NT*	NT*	NT*	31.5 ± 0.50

NT* = not tested

Moderate to good antibacterial results were observed for all tested compounds, the products being less active than specific agents used as positive controls (Table IV). The best results were obtained for products having halogens (F, Cl, Br) in para position of the benzene ring whether the compounds were low-molecular-weight or polymeric ones. Their enhanced antimicrobial activity could be explained by the existence of a supplementary partial positive charge on benzene ring, induced by the presence of electron-withdrawing substituents (F, Cl, Br) bound to the aromatic ring. The improvement of the antimicrobial activity has also been observed for other polymers which contained halogen atoms in their chemical structure [33, 60]. The stronger electron-withdrawing capacity of the substituent (F > Cl > Br), the enhanced the antibacterial activity. The antifungal activity was generally higher than the antibacterial one for each product and the occurrence of strong electron-withdrawing substituents

enhanced the antifungal properties as in the case of antibacterial activity (Table IV).

Antimicrobial activity was greater for polymers compared to their corresponding 1,2,3-triazole derivatives due to the occurrence of an increased local concentration of N-heterocycle groups which augmented the ionic and hydrophobic interactions between the polymer and lipid bilayer of bacteria or fungi membrane. The same antimicrobial behaviour was observed for hydrophobically modified acrylate-based polymers and their corresponding monomers [58]. Polymers, having the best qualitative antimicrobial results, were further evaluated by using broth microdilution method which provided the minimum inhibitory concentrations (MIC), minimal bactericidal concentration (MBC) and the minimal fungicidal concentration (MFC) (Table V). The self-aggregation process of substrate is an important factor which influenced the antimicrobial activity by changing the membrane wholeness of the micro-

organisms. MIC values were higher than CAC values which denoted those above-mentioned polymers were

active only in their self-assembled form for both antibacterial and antifungal activity.

Table V

MIC and MBC/MFC values of tested polymers

Compound	<i>S. aureus</i> ATCC 25923		<i>C. albicans</i> ATCC 90028	
	MIC (mg/mL)	MBC (mg/mL)	MIC (mg/mL)	MFC (mg/mL)
2b	2.00	4.00	0.312	0.65
2c	2.50	5.00	0.625	1.75
2d	2.5	> 5.00	1.25	2.85
Ciprofloxacin	1 ^a	2 ^a	NT*	NT*
Fluconazole	NT*	NT*	8 ^a	16 ^a

^a Values are expressed in µg/mL; NT* = not tested

This behaviour could also be seen for other macro-molecular amphiphilic compounds for which the antimicrobial activity became effective when the concentration was above CAC [44, 58]. The capacity of self-aggregation of dextran esters (Table II) correlated with their antimicrobial activity (Table V). Thus, the increase of self-association ability of the polymers determined a decrease of their bactericidal and fungicidal properties. MIC values of dextran amphiphilic esters were of the same order of magnitude with values reported for other non-ionic carbohydrate-derived containing 1,2,3-triazole moieties. Thus, for 4-sulfanilamido substituted-1,2,3-triazoles conjugated with monosaccharides were recorded MIC values between 0.08 - 5 mg/mL against *S. aureus* and 0.31 - 5 mg/mL against *C. albicans* [6] while for other 1,2,3-triazoles glycoside, MIC values were between 5 - 10 mg/mL against *S. aureus* and *C. albicans* [16].

An antimicrobial agent is considered to be bactericidal and/or fungicidal if the ratios MBC/MIC and/or MFC/MIC ≤ 4 [56]. The tested polymers (Table V) proved to have both bactericidal and fungicidal activity, as their ratios satisfied above-mentioned condition.

Conclusions

Hydrophobically modified dextran esters having 1,2,3-triazole derivatives as pendant groups were obtained by a one-pot reaction. Structural characteristics of the polymers were revealed by elemental analysis, XPS, FTIR and ¹³C NMR spectroscopy. Antimicrobial susceptibility tests showed that the polymers having electron-withdrawing substituents in their structure revealed the best antimicrobial activity while broth microdilution method proved bactericidal and fungicidal properties for this type of polysaccharide esters. The comparison between CAC and MIC values, proved the correlation between self-organizing capacity of dextran esters and their antimicrobial activity.

Conflict of interest

The authors declare no conflict of interest.

References

1. Agalave SG, Maujan SR, Pore VS, Click chemistry: 1,2,3-triazoles as pharmacophores. *Chem Asian J.*, 2011; 6(10): 2696-718.
2. Akolkar SV, Nagargoje AA, Krishna VS, Sriram D, Sangshetti JN, Damaled M, Shingate BB, New N-phenylacetamide-incorporated 1,2,3-triazoles: [Et3NH][OAc]-mediated efficient synthesis and biological evaluation. *RSC Adv.*, 2019; 9: 22080-22091.
3. Ashok D, Chiranjeevi P, Kumar AV, Sarasija M, Krishna VS, Sriram D, Balasubramanian S, 1,2,3-Triazole-fused spirochromenes as potential anti-tubercular agents: Synthesis and biological evaluation. *RSC Adv.*, 2018; 8: 16997-17007.
4. Ashok D, Gundu S, Aamate VK, Devulapally MG, Bathini R, Manga V, Dimers of coumarin-1,2,3-triazole hybrids bearing alkyl spacer: Design, microwave-assisted synthesis, molecular docking and evaluation as antimycobacterial and antimicrobial agents. *J Mol Struct.*, 2018; 1157: 312-321.
5. Avula SK, Khan A, Rehman NU, Anwar MU, Al-Aabri Z, Wadood A, Riaz M, Csuk R, Al-Harrasi A, Synthesis of 1H-1,2,3-triazole derivatives as new α -glucosidase inhibitors and their molecular docking studies. *Bioorg Chem.*, 2018; 81: 98-106.
6. Ay K, Ispartaloğlu B, Halay E, Synthesis and antimicrobial evaluation of sulfanilamide- and carbohydrate-derived 1,4-disubstituted-1,2,3-triazoles via click chemistry. *Med Chem Res.*, 2017; 26: 1497-1505.
7. Barzic AI, Ioan S, Antibacterial drugs-From basic concepts to complex therapeutic mechanisms of polymer systems. In: Concepts, Compounds and the Alternatives of Antibacterials, V. Bobbarala (Ed.); Science, Technology and Medicine, London, UK, 2015; 1-28.
8. Batra N, Rajendran V, Agarwal D, Wadi I, Ghosh PC, Gupta RD, Nath M, Synthesis and antimalarial evaluation of [1,2,3]-triazole-tethered sulfonamide-berberine hybrids. *ChemistrySelect*, 2018; 3: 9790-9793.
9. Cheng H, Wan J, Lin M-I, Liu Y, Lu X, Liu J, Xu Y, Chen J, Tu Z, Cheng Y-SE, Design, synthesis, and *in vitro* biological evaluation of 1H-1,2,3-triazole-4-carboxamide derivatives as new anti-influenza A agents targeting virus nucleoprotein. *J Med Chem.*, 2012; 55: 2144-2153.

10. Chu X-M, Wang C, Wang W-L, Liang L-L, Liu W, Gong K-K, Sun K-L, Triazole derivatives and their antiplasmodial and antimalarial activities. *Eur J Med Chem.*, 2019; 166: 206-223.
11. CLSI. Method for Antifungal Disk Diffusion Susceptibility Testing of Yeasts. CLSI guideline M44. In: Clinical and Laboratory Standards Institute, 3rd ed., Wayne PA (Ed.), 2018.
12. CLSI. Performance Standards for Antimicrobial Susceptibility Testing, Clinical and Laboratory Standards Institute, CLSI supplement M100. In: Clinical and Laboratory Standards Institute, 32nd ed., Wayne PA (Ed.), 2022.
13. Dai ZC, Chen YF, Zhang M, Li SK, Yang TT, Shen L, Wang JX, Qian SS, Zhue HL, Ye YH, Synthesis and antifungal activity of 1,2,3-triazole phenylhydrazone derivatives. *Org Biomol Chem.*, 2015; 13: 477-486.
14. El Malah T, Nour HF, Dehbi O, Abdel-Megeid FME, Essam El-Din Mahmoud A, Ali MM, Soliman SM, Click synthesis, anticancer activity and molecular docking studies on pyridazinone scaffolds. *Curr Org Chem.*, 2018; 22: 2300-2307.
15. El Malah T, Nour HF, Nayl AA, Elkhatab RA, Abdel-Megeid FME, Ali MM, Anticancer evaluation of tris(triazolyl)triazine derivatives generated via click chemistry. *Aust J Chem.*, 2016; 69: 905-910.
16. El Malah T, Nour HF, Satti AAE, Hemdan BA, El-Sayed WA, Design, Synthesis, and Antimicrobial Activities of 1,2,3-Triazole Glycoside Clickamers. *Molecules*, 2020; 25(4): 790: 1-17.
17. El-Sayed WA, Khalaf HS, Mohamed SF, Hussien HA, Kutkat OM, Amr A-EE, Synthesis and antiviral activity of 1,2,3-triazole glycosides based substituted pyridine via click cycloaddition. *Russ J Gen Chem.*, 2017; 87: 2444-2453.
18. Ferreira SB, Sodero ACR, Cardoso MFC, Lima ES, Kaiser CR, Silva FP, Ferreira VF, Synthesis, biological activity, and molecular modeling studies of 1H-1,2,3-triazole derivatives of carbohydrates as α -glucosidases inhibitors. *J Med Chem.*, 2010; 53: 2364-2375.
19. Głowacka IE, Andrei G, Schols D, Snoeck R, Piotrowska DG, Phosphonylated acyclic guanosine analogues with the 1,2,3-triazole linker. *Molecules*, 2015; 20: 18789-18807.
20. Goud GL, Ramesh S, Ashok D, Reddy VP, Yogeewari P, Sriram D, Saikrishna B, Manga V, Design, synthesis, molecular-docking and antimycobacterial evaluation of some novel 1,2,3-triazolyl xanthenones. *Med Chem Commun.*, 2017; 8: 559-570.
21. Gupta RS, What are archaeobacteria: life's third domain or monoderm prokaryotes related to Gram-positive bacteria? A new proposal for the classification of prokaryotic organisms. *Mol Microbiol.*, 1998; 29(3): 695-707.
22. Gupta RS, The natural evolutionary relationships among prokaryotes. *Crit Rev Microbiol.*, 2000; 26(2): 111-131.
23. Hoque J, Akkapeddi P, Yarlagadda V, Uppu D, Kumar P, Haldar J, Cleavable Cationic Antibacterial Amphiphiles: Synthesis, Mechanism of Action, and Cytotoxicities. *Langmuir*, 2012; 28(33): 12225-12234.
24. Huang RZ, Liang GB, Li MS, Fang YL, Zhao SF, Zhou MM, Liao ZX, Sun J, Wang HS, Synthesis and discovery of asiatic acid based 1,2,3-triazole derivatives as antitumor agents blocking NF- κ B activation and cell migration. *Med Chem Commun.*, 2019; 10: 584-597.
25. Jiang X, Wu G, Zalloum WA, Meuser ME, Dick A, Sun L, Chen C-H, Kang D, Jing L, Jia R, Discovery of novel 1,4-disubstituted 1,2,3-triazole phenyl-alanine derivatives as HIV-1 capsid inhibitors. *RSC Adv.*, 2019; 9: 28961-28986
26. Jingmou Y, Yunfeng Zh, Wencong Ch, Jin R, Lifang Zh, Lu L, Gan L, Hao H, Preparation, Characterization and Evaluation of α -Tocopherol Succinate-Modified Dextran Micelles as Potential Drug Carriers. *Materials*, 2015; 8: 6685-6696.
27. Jorgensen JH, Ferraro MJ, Antimicrobial susceptibility testing: a review of general principles and contemporary practices. *Clin Infect Dis.*, 2009; 49(11): 1749-1755.
28. Kassem AF, Abbas EMH, El-Kady DS, Awad HM, El-Sayed WA, Synthesis, docking studies and anticancer activity of new tetrazolyl- and (triazolyl)thiazole glycosides and acyclic analogs. *Mini-Rev Med Chem.*, 2019; 19: 933-948.
29. Kaushik CP, Luxmi R, Kumar M, Singh D, Kumar K, Pahwa A, One-pot facile synthesis, crystal structure and antifungal activity of 1,2,3-triazoles bridged with amine-amide functionalities. *Synth Commun.*, 2019; 49: 118-128.
30. Kenawy ER, Worley SD, Broughton R, The chemistry and applications of antimicrobial polymers: A state-of-the-art review. *Biomacromolecules*, 2007; 8: 1359-1384.
31. Khaldi Z, Besse C, Nzambe Ta Keki JK, Ouk T-S, Gloaguen V, Zerrouki R, Synthesis, characterization, and antibacterial activities of a new lignocellulosic material carrying aryl triazole moiety. *Polym Adv Technol.*, 2019; 30: 344-350.
32. Khalil H, El Malah T, Abd El Maksoud AI, El Halfawy I, El Rashedy AA, El Hefnawy M, Identification of novel and efficacious chemical compounds that disturb influenza A virus entry *in vitro*. *Front Cell Infect Microbiol.*, 2017; 7: 304: 1-11.
33. Lal K, Yadav P, Kumar A, Kumar A, Paul AK, Design, synthesis, characterization, antimicrobial evaluation and molecular modeling studies of some dehydroacetic acid-chalcone-1,2,3-triazole hybrids, *Bioorg Chem.*, 2018; 77: 236-244.
34. Malik B, Bhattacharyya S, Antibiotic drug-resistance as a complex system driven by socio-economic growth and antibiotic misuse. *Sci Rep.*, 2019; 9: 9788: 1-12.
35. Mallemula VR, Sanghai NN, Himabindu V, Synthesis and characterization of antibacterial 2-(pyridin-3-yl)-1H-benzo[d]imidazoles and 2-(pyridin-3-yl)-3H-imidazo[4,5-b]pyridine derivatives. *Res Chem Intermed.*, 2015; 41: 2125-2138.
36. Mechken KA, Menouar M, Belkhdja M, Saidi-Besbes S, Synthesis, surface properties and bioactivity of novel 4-Substituted 1,2,3-Triazole quaternary ammonium surfactants. *J Mol Liq.*, 2021; 338: 116775: 1-11.
37. Mohammed I, Kummetha IR, Singh G, Sharova N, Lichinchi G, Dang J, Stevenson M, Rana TM, 1,2,3-Triazoles as amide bioisosteres: Discovery of a new class of potent HIV-1 Vif antagonists. *J Med Chem.*, 2016; 59: 7677-7682.
38. Naaz F, Pallavi MCP, Shafic S, Mulakayala N, Yar MS, Kumar HMS, 1,2,3-triazole tethered Indole-3-

- glyoxamide derivatives as multiple inhibitors of 5-LOX, COX-2 & tubulin: Their anti-proliferative & anti-inflammatory activity. *Bioorg Chem.*, 2018; 81: 1-20.
39. Ochman H, Lawrence JG, Groisman EA, Lateral gene transfer and the nature of bacterial innovation. *Nature*, 2000; 405: 299-304.
 40. Oubella A, Bimoussa A, N'ait Oussidi A, Fawzi M, Auhmani A, Morjani H, Riahi A, Esseffar M, Parish C, Ait Itto MY, New 1,2,3-Triazoles from (R)-Carvone: Synthesis, DFT Mechanistic Study and *In Vitro* Cytotoxic Evaluation. *Molecules*, 2022; 27(3):769: 1-18.
 41. Phatak PS, Bakale RD, Dhupal ST, Dahiwade LK, Choudhari PB, Krishna VS, Sriram D, Haval KP, Synthesis, antitubercular evaluation and molecular docking studies of phthalimide bearing 1,2,3-triazoles. *Synth Commun.*, 2019; 49: 2017-2028.
 42. Pogaku V, Krishna VS, Balachandran C, Rangan K, Sriram D, Aoki S, The design and green synthesis of novel benzotriazolopyridinylspirooxindole rolizidines: Antimycobacterial and antiproliferative studies. *New J Chem.*, 2019; 43: 17511-17520.
 43. Porta EOJ, Verdaguer IB, Perez C, Banchio C, Ferreira de Azevedo M, Katzin AM, Labadie GR, Repositioning Salirasib as a new antimalarial agent. *Med Chem Commun.*, 2019; 10: 1599-1605.
 44. Qiao Y, Yang C, Coody DJ, Ong ZY, Hedrick JL, Yang YY, Highly dynamic biodegradable micelles capable of lysing Gram-positive and Gram-negative bacterial membrane. *Biomaterials*, 2012; 33(4): 1146-1153.
 45. Rao PS, Kurumurthy C, Veeraswamy B, Kumar GS, Poomachandra Y, Kumar CG, Vasamsetti SB, Kotamraju S, Narsaiah B, Synthesis of novel 1,2,3-triazole substituted-N-alkyl/aryl nitrene derivatives, their anti-inflammatory and anticancer activity. *Eur J Med Chem.*, 2014; 80: 184-191.
 46. Reddyrajula R, Dalimba U, Kumar SM, Molecular hybridization approach for phenothiazine incorporated 1,2,3-triazole hybrids as promising antimicrobial agents: Design, synthesis, molecular docking and in silico ADME studies. *Eur J Med Chem.*, 2019; 168: 263-282.
 47. Reichardt C, Solvatochromic Dyes as Solvent Polarity Indicators. *Chem Rev.*, 1994; 94: 2319-2358.
 48. Rostovtsev VV, Green LG, Fokin VV, Sharpless KB, A stepwise Huisgen cycloaddition process: Copper(I)-catalyzed regioselective "Ligation" of azides and terminal alkynes. *Angew Chem Int Ed.*, 2002; 41: 2596-2599.
 49. Saeedi M, Mohammadi-Khanaposhtani M, Pourrabia P, Razzaghi N, Ghadimi R., Imanparast S, Faramarzi MA, Bandarian F, Esfahani EN, Safavi M, Design and synthesis of novel quinazolinone-1,2,3-triazole hybrids as new antidiabetic agents: *In vitro* α -glucosidase inhibition, kinetic, and docking study. *Bioorg Chem.*, 2019; 83: 161-169.
 50. Sajja Y, Vanguru S, Vulupala HR, Bantu R, Yogeswari P, Sriram D, Nagarapu L, Design, synthesis and *in vitro* antituberculosis activity of benzo [6,7]cyclohepta [1-b]pyridine-1,2,3-triazole derivatives. *Bioorg Med Chem.*, 2017; 27(23): 5119-5121.
 51. Stanciu MC, Belei D, Bicu E, Tuchilus CG, Nichifor M, Novel amphiphilic dextran esters with antimicrobial activity. *Int J Biol Macromol.*, 2020; 150: 746-755. 2017; 27(23): 5119-5121.
 52. Tan W, Li Q, Wang H, Liu Y, Zhang J, Dong F, Guo Z, Synthesis, characterization, and antibacterial property of novel starch derivatives with 1,2,3-triazole. *Carbohydr Polym.*, 2016; 142: 1-7.
 53. Thomas CM, Nielsen KM, Mechanisms of, and barriers to, horizontal gene transfer between bacteria. *Nat Rev Microbiol.*, 2005; 3:711-721.
 54. Tolan HEM, El-Sayed WA, Tawfek N, Abdel-Megeid FME, Kutkat OM, Synthesis and anti-H5N1 virus activity of triazole- and oxadiazole-pyrimidine hybrids and their nucleoside analogs. *Nucleosides Nucleotides Nucleic Acids*, 2019; 39(5): 649-670.
 55. Tornøe CW, Christensen C, Meldal M, Peptidotriazoles on solid phase: [1,2,3]-Triazoles by regioselective copper(I)-catalyzed 1,3-dipolar cycloadditions of terminal alkynes to azides. *J. Org Chem.*, 2002; 67: 3057-3064.
 56. Tuchilus CG, Nichifor M, Mocanu G, Stanciu MC, Antimicrobial activity of chemically modified dextran derivatives. *Carbohydr. Polym.*, 2017; 161: 181-186.
 57. von Wintersdor CJH, Penders J, van Niekerk JM, Mills ND, Majumder S, van Alphen LB, Savelkoul PHM, Wolfs PFG, Dissemination of antimicrobial resistance in microbial ecosystems through horizontal gene transfer. *Front Microbiol.*, 2016; 7: 173: 1-10.
 58. Wang H, Shi X, Yu D, Zhang J, Yang G, Cui Y, Sun K, Wang J, Yan H, Antibacterial Activity of Geminized Amphiphilic Cationic Homopolymers. *Langmuir*, 2015; 31(50): 13469-13477.
 59. Xue Y, Xiao H, Zhang Y, Antimicrobial polymeric materials with quaternary ammonium and phosphonium salts. *Int J Mol Sci.*, 2015; 16: 3626-3655.
 60. Yadav P, Lal K, Kumar L, Kumar A, Kumar A, Paul AK, Synthesis, crystal structure and antimicrobial potential of some fluorinated chalcone-1,2,3-triazole conjugates. *Eur J Med Chem.*, 2018; 155: 263-274.
 61. Yijuan Zh, Ping L, Hong P, Lanlan L, Manyi J, Nan S, Ce W, Lintao C, Yifan M, Retinal-conjugated pH-sensitive micelles induce tumor senescence for boosting breast cancer chemotherapy. *Biomaterials*, 2016; 83: 219-232.
 62. Yong-Zhong D, Qi W, Hong Y, Fu-Qiang H, Synthesis and antitumor activity of stearate-g-dextran micelles for intracellular doxorubicin delivery. *ACS Nano*, 2010; 4: 6894-6902.
 63. Zhang S, Ding S, Yu J, Chen X, Lei Q, Fang W, Antibacterial Activity, *in Vitro* Cytotoxicity, and Cell Cycle Arrest of Gemini Quaternary Ammonium Surfactants. *Langmuir*, 2015; 31(44): 12161-12169.
 64. Zhou Z, Liu T, Wu G, Kang D, Fu Z, Wang Z, De Clercq E, Pannecouque C, Zhan P, Liu X, Targeting the hydrophobic channel of NNIBP: Discovery of novel 1,2,3-triazole-derived dihydropyrimidines as novel HIV-1 NNRTIs with high potency against wild-type and K103N mutant virus. *Org Biomol Chem.*, 2019; 17: 3202-3321.